Hindawi
Mathematical Problems in Engineering
Volume 2019, Article ID 8291063, 13 pages
https://doi.org/10.1155/2019/8291063

Research Article

An Efficient Approximation for Nakagami-*m* Quantile Function Based on Generalized Opposition-Based Quantum Salp Swarm Algorithm

Hongyuan Gao, Yangyang Hou, Shibo Zhang, and Ming Diao

College of Information and Communication Engineering, Harbin Engineering University, No. 145, Nantong Street, Nangang District, Harbin 150001, China

Correspondence should be addressed to Hongyuan Gao; gaohongyuan@hrbeu.edu.cn

Received 26 April 2019; Revised 9 July 2019; Accepted 28 July 2019; Published 14 August 2019

Academic Editor: Łukasz Jankowski

With the further research in communication systems, especially in wireless communication systems, a statistical model called Nakagami-*m* distribution appears to have better performance than other distributions, including Rice and Rayleigh, in explaining received faded envelopes. Therefore, the Nakagami-*m* quantile function plays an important role in numerical calculations and theoretical analyses for wireless communication systems. However, it is quite difficult to operate numerical calculations and theoretical analyses because Nakagami-*m* quantile function has no exact closed-form expression. In order to obtain the closed-form expression that is able to fit the curve of Nakagami-*m* quantile function as well as possible, we adopt the method of curve fitting in this paper. An efficient expression for approximating the Nakagami-*m* quantile function is proposed first and then a novel heuristic optimization algorithm—generalized opposition-based quantum salp swarm algorithm (GO-QSSA)—which contains quantum computation, intelligence inspired by salp swarm and generalized opposition-based learning strategy in quantum space, to compute the coefficients of the proposed expression. Meanwhile, we compare GO-QSSA with three swarm intelligence algorithms: artificial bee colony algorithm (ABC), particle swarm optimization algorithm (PSO), and salp swarm algorithm (SSA). The comparing simulation results reveal that GO-QSSA owns faster convergence speed than PSO, ABC, and SSA. Moreover, GO-QSSA is capable of computing more accurately than traditional algorithms. In addition, the simulation results show that compared with existing curve-fitting-based methods, the proposed expression decreases the fitting error by roughly one order of magnitude in most cases and even higher in some cases. Our approximation is proved to be simple and efficient.

1. Introduction

It is well known that radiowave propagation is complicated under the environment of wireless channels and various effects exert different impacts on the characteristics of radiowave propagation. Considerable research focusing on building the statistical models and characterizing these effects has been undertaken. Multipath fading is of great significance among the effects and is caused by the combination of various signal components containing randomly diffracted, reflected, delayed, and scattered components. There are different models used under different radio propagation environments, such as Rayleigh, Rice, Hoyt, and Weibull distributions [1], and these four models are capable of describing the corresponding statistical characterization of the envelope caused by multipath fading. Propagation paths can be modelled by Rayleigh distribution if line-of-sight (LOS) component does not exist [2]. Propagation paths containing many random weaker components and one strong direct LOS component are usually modelled by the Rice distribution, such as suburban land-mobile and microcellular urban components with the first resolvable LOS paths [3]. Among these models, the best statistical model that is capable of defining different multipath fading conditions is the Nakagami-*m* distribution. Nakagami-*m* distribution is diffusely adopted in wireless communication systems due to its two main advantages. One is its flexibility feature; in fact, Rayleigh distribution is essentially the special case when the fading parameter of Nakagami-*m* distribution is

set as 1 [1]. Furthermore, the channel modelled with Nakagami-m distribution can converge to a nonfading AWGN channel, and different parameters even make it a close approximation to the Hoyt and Rice distribution. Another significant feature is that the Nakagami-m distribution is a perfect statistical model to fit scintillating ionospheric radio links, indoor-mobile multipath propagation, and land-mobile multipath propagation [4–8].

Numerical calculations and theoretical analyses in wireless communications under the Nakagami-m fading environment can be operated with inverse and normal CDFs. However, it is difficult to utilize Nakagami-m quantile function firsthand to operate these calculations because the exact closed-form expression of Nakagami-m quantile function does not exist. In recent years, a new method to approximate the quantile function of Nakagami-m distribution by dint of the curve-fitting method has been illustrated, and scholars have utilized several metaheuristic optimization algorithms to compute the coefficients of their expressions correspondingly, such as the genetic algorithm [4], backtracking search optimization algorithm [5], and artificial bee colony optimization [6].

In this paper, an expression with lower computational complexity and better performance for approximating the Nakagami-m quantile function is proposed firstly, and then we propose a novel algorithm called generalized opposition-based quantum salp swarm algorithm (GO-QSSA) to compute coefficients of the proposed expression. Here, we propose the generalized opposition-based learning strategy in quantum space, and we apply it to QSSA. Finally, our simulation results under different parameters of Nakagami-m quantile function prove the accuracy of the proposed expression and the efficiency of GO-QSSA.

The contributions of our work are summarized as follows:

(1) We propose a briefer and more efficient expression to approximate the quantile function of the Nakagami-m model. Compared with the approaches in [9], our curve-fitting-based method is superior both in the computational complexity and the number of expression coefficients. Among all the existing curve-fitting-based methods in [4], the fitting equation is characterized by a division comprised of two polynomial equations and five parameters in total. However, the expression proposed in this paper is just a polynomial containing three simple elementary functions and four parameters which we need to compute. Compared with References [4–6], our simulation results prove the strengths of our approximation.

(2) We propose the generalized opposition-based learning strategy in quantum space, which is first proposed in the literature. Meanwhile, we apply this strategy to QSSA to improve its convergence speed.

(3) We propose the quantum intelligent algorithm which is named GO-QSSA. It is the first time that quantum swarm intelligence is combined with salp swarm algorithm and quantum evolutionary strategy, and the results prove the accuracy of the proposed expression and the efficiency of GO-QSSA.

The remaining part is structured as follows: Section 2 is the related work. In Section 3, the Nakagami-m model and approximation problem model are introduced. In Section 4, the methodology is illustrated, the expression proposed to approximate Nakagami-m quantile function is presented, we propose generalized opposition-based quantum salp swarm algorithm, and then we use GO-QSSA to solve this problem. The enormous simulation results and numerical analyses are shown in Section 5. In Section 6, finally, the main work of this paper is summarized.

2. Related Work

Many researchers have focused on numerical calculations and theoretical analyses under the Nakagami-m fading environment with its inverse and normal CDFs. Das et al. in [8] considered the mobility of nodes and derived the CDF and PDF of the received power at the mobile nodes in the Nakagami-m fading environment. Eventually, they deduced the expressions for average bit error rate (BER) and coverage probability. In [10], a finite network of drones (also called unmanned aerial vehicles, UAVs) serving a given region was considered, and the downlink coverage probability was derived assuming all wireless links were compliant with Nakagami-m distribution. Hou et al. [11] studied the outage performance considering Nakagami-m fading with different fading parameters and the fixed power allocation of non-orthogonal multiple access (NOMA). In addition, a communication network assisted by a wireless powerbeacon (PB) was investigated in [12]. In this network, one receiver, multiple transmitters, and multiple PBs were considered. These transmitters harvest energy from the PBs and transmit their data, respectively, to the receiver. Fading coefficients were assumed to be Nakagami-m random variables during the transmission. The authors derived the expression of achievable throughput and an approximated closed-form expression of throughput when the signal-to-noise ratio was high. Moreover, in [13], under the Nakagami-m and Hoyt fading channels, analytical expressions of the symbol error rate (SER) system were deduced, and the simulation results confirmed the GFDM/OQAM model proposed by the authors. These illustrations above enlighten us to the fact that the Nakagami-m quantile function is vital to calculate some performance indicators of wireless communication systems such as BER, throughput, coverage probability, and outage probability. However, it is difficult to utilize Nakagami-m quantile function firsthand to operate these calculations because the exact closed-form expression for Nakagami-m quantile function does not exist. Some methods have been proposed to acquire the approximated Nakagami-m quantile function such as Gaussian distribution and Hastings' approach [9], whereas these approaches have some defects including their high computational complexity and the complex form of their expressions.

In recent years, a new method to approximate the quantile function of Nakagami-m distribution by dint of the curve-fitting method has been illustrated, and scholars have utilized several metaheuristic optimization algorithms to compute the coefficients of their expressions

correspondingly, such as the genetic algorithm [4], backtracking search optimization algorithm [5], and artificial bee colony optimization [6]. Bilim and Develi[4] proposed an expression consisting of a cubic polynomial and a linear polynomial and then used genetic algorithm to compute its total five coefficients. Kabalci [5, 6] investigated a more concise expression with four coefficients. Meanwhile, he adopted backtracking search optimization algorithm and artificial bee colony optimization to solve this curve-fitting problem, respectively. In this paper, a novel and more efficient expression and a novel heuristic algorithm called GO-QSSA are proposed to approximate the Nakagami-m quantile function. Related theoretical background and methodology will be illustrated next.

3. Theoretical Background and Problem Modelling

3.1. Nakagami-m Model. Concepts and properties have been interpreted in [9] in detail. In this section, for clarity, we restate the concepts and main properties of Nakagami-m distribution. Meanwhile, the method for calculating Nakagami-m quantile function is presented in detail. Nakagami-m distribution has two parameters: a fading parameter, m, denoting the fading effect of the wireless communication channel, and a scaling parameter, Ω, controlling spread. Assuming S is a random variable complying with the Nakagami-m distribution, its PDF is defined as follows:

$$f_S(s; m, \Omega) = \frac{2m^m s^{2m-1}}{\Gamma(m)\Omega^m} e^{-(m/\Omega)s^2}, \quad \forall s > 0,\ m \geq \frac{1}{2},\ \Omega > 0, \tag{1}$$

where $\Gamma(\cdot)$ is the symbol of the Gamma function. The fading parameter m and scaling parameter Ω can also be estimated as

$$m = \frac{\left(E\left[S^2\right]\right)^2}{\operatorname{var}\left[S^2\right]}, \qquad \Omega = E\left[S^2\right], \tag{2}$$

where $\operatorname{var}[\cdot]$ and $E[\cdot]$, respectively, denote variance and expectation operators.

The Nakagami-m distribution shows the largest range of AF (amount of fading) among all the distributions describing multipath fading characterization considered in [1]. It contains two special cases, one is the one-sided Gaussian distribution when the fading parameter is set as 0.5, and the other is Rayleigh distribution when the fading parameter is set as 1.0. Furthermore, when $m > 1$, it is close to the Rice distribution; when $m < 1$, it is capable of approximating the Hoyt distribution. Finally, the Nakagami-m distribution is regarded as the best statistic model to fit scintillating ionospheric radio links, indoor-mobile multipath propagation, and land-mobile multipath propagation.

According to the relationship between PDF and CDF in probability theory, the CDF is defined as

$$F_S(s; m, \Omega) = \int_0^s f_S(w; m, \Omega)\, dw. \tag{3}$$

Hence, the quantile function of Nakagami-m can be acquired by dint of the CDF of Nakagami-m distribution:

$$F_S(s; m, \Omega) = \int_0^{s(u)} \frac{2m^m w^{2m-1}}{\Gamma(m)\Omega^m} e^{-(m/\Omega)w^2}\, dw, \tag{4}$$

where u is defined as

$$u = 1 - e^{-\left(s^2/2\sigma^2\right)}, \tag{5}$$

where σ^2 is the second moment of S and $s(u)$ is a transformation function. Finally, we acquire the Nakagami-m quantile function $F_S^{-1}(u; m, \Omega)$ with the variable transformation u, However, it is obvious that the consequent expression of Nakagami-m quantile function involves a complex integral. Moreover, it has been proven that the exact closed-form expression for the Nakagami-m quantile function does not exist except when $m = 1$ [1, 9]. Therefore, we propose a novel expression to approximate the Nakagami-m quantile function in Section 3.2.

3.2. Modelling for Approximating Nakagami-m Quantile Function. We have obtained the exact value of the Nakagami-m quantile function $F_S^{-1}(u; m, \Omega)$ for a certain u in the former section, and in fact, u represents the Nakagami-m CDF value. We use $F_{S_{(\text{proposed})}}^{-1}(u)$ to denote our proposed expression for approximating the Nakagami-m quantile function, which will be shown in Section 4. Assuming that the expression entirely contains D coefficients denoted as $\varrho_1, \varrho_2, \ldots, \varrho_D$, respectively, we aim at computing the optimal coefficients satisfying the best curve-fitting performance. A generally used criterion to evaluate the performance of a fitting equation is the root-mean-square error (RMSE). Here, we use the RMSE to measure the approximation error between the exact value of Nakagami-m quantile function $F_S^{-1}(u; m, \Omega)$ and the value predicted by the proposed expression $F_{S_{(\text{proposed})}}^{-1}(u)$. In this paper, we use $\zeta(\varrho_1, \varrho_2, \ldots, \varrho_D)$ to denote the RMSE and our fitness function; then, the RMSE is calculated as

$$\zeta(\varrho_1, \varrho_2, \ldots, \varrho_D) = \sqrt{\frac{\sum_{i=1}^{N}\left(F_{S_{(\text{proposed})}}^{-1}(u_i) - F_S^{-1}(u_i; m, \Omega)\right)^2}{N}}, \tag{6}$$

where u_i denotes the ith sampling point, N is the number of sampling points, $F_{S_{(\text{proposed})}}^{-1}(u_i)$ is the approximation value at u_i, and $F_S^{-1}(u_i; m, \Omega)$ is the exact value of Nakagami-m quantile function at u_i. Here, we can model the curve fitting problem as

$$\varrho_1^*, \varrho_2^*, \ldots, \varrho_D^* = \arg \min_{\varrho_1, \varrho_2, \ldots, \varrho_D} \zeta(\varrho_1, \varrho_2, \ldots, \varrho_D) \quad \text{subject to :} \quad \rho_j \leq c_j \leq \varphi_j, \tag{7}$$

where ρ_j indicates the lower bound of the jth coefficient and φ_j indicates the upper bound of the jth coefficient, respectively, and $\varrho_1^*, \varrho_2^*, \ldots, \varrho_D^*$ represent optimal coefficients which enable the RMSE to achieve the minimum.

So far, we have modelled the approximation problem. Next, we will expound the methodology on both expression and algorithm aspects.

4. Methodology

There are two main aspects to be addressed when solving this problem. One is the expression designed to approximate Nakagami-m quantile function, which should be not only brief but also efficient, that is to say, the proposed expression is supposed to minimize the RMSEs. Meanwhile, it should not increase excessive computational complexity; the other is the heuristic algorithm adopted to calculate coefficients of the expression. The algorithm needs to satisfy the requirements of faster convergence speed and higher accuracy. Here, we propose GO-QSSA to achieve this goal.

4.1. Expression for Approximating Nakagami-m Quantile Function. It is well known that the foremost aspect is the mathematical expression for a curve-fitting problem, and as mentioned above, we propose a new approximation model with higher accuracy as follows:

$$F^{-1}_{S_{(\text{proposed})}}(u) = a\tanh^{-1}(u) + bu^{c}\exp(du), \tag{8}$$

where $\tanh^{-1}(\cdot)$ is the inverse hyperbolic tangent function, $\exp(\cdot)$ is the exponential function, and a, b, c, and d are coefficients.

In order to compare clearly with available approximations previously reported in the literature, we introduce them briefly. Beaulieu and Cheng [9] followed Hastings' approach and proposed an approximation as follows:

$$G(u) = \tau + \frac{\varpi_1\tau + \varpi_2\tau^2 + \varpi_3\tau^3}{1 + \varpi_4\tau + \varpi_5\tau^2}, \tag{9}$$

where $\tau = \left(\sqrt{\ln(1/(1-u))}\right)^{(1/m)}$ is an ancillary variable, m is the fading parameter, $\varpi_1, \varpi_2, \varpi_3, \varpi_4$, and ϖ_5 are coefficients, and $G(u)$ represents an approximated value of the Nakagami-m quantile function. Apparently, this approximation, containing two equations and five coefficients, is quite complex. In order to simplify the expression, Bilim and Develi [4] applied the curve fitting method to this problem, and they proposed the following expression:

$$F^{-1}_{B_{(\text{proposed})}}(u) = \frac{\kappa_1 u + \kappa_2}{u^3 + \kappa_3 u^2 + \kappa_4 u + \kappa_5}. \tag{10}$$

This is much simpler than (9), although it also has five coefficients, κ_1, κ_2, κ_3, κ_4, and κ_5. Later, Kabalci [5, 6] investigated a more concise expression as follows:

$$F^{-1}_{K_{(\text{proposed})}}(u) = k_1\tanh^{-1}(u)\exp(k_2 u) + k_3\exp(k_4 u). \tag{11}$$

There are only four coefficients in this expression, with an inverse hyperbolic tangent function and two exponential functions. However, in practice, equation (11) does not always have better performance than (10) under various situations, which can be observed in those figures of simulation results in their papers. The defects of (11) motivate us to further investigate this problem. To some extent, the expression we propose, (8), is inspired from (11). The inverse hyperbolic tangent function is the core for both expressions (8) and (11). The deeper cause for the choice of the inverse hyperbolic tangent function is that this function is similar in shape to the Nakagami-m quantile function, which is illustrated in Figures 1(a) and 1(b). It can be easily observed that the Nakagami-m quantile function has the same trend with the inverse hyperbolic tangent function in the domain $[0, 1)$, when the fading parameter m is small, and when m grows, the Nakagami-m quantile function has the same trend with the inverse hyperbolic tangent function in the whole domain $(-1, 1)$. Hence, it is convenient to adopt the inverse hyperbolic tangent function as the basis of the expression for approximating the Nakagami-m quantile function; meanwhile, we compensate for the deviations between the values of inverse hyperbolic tangent function and the exact values of Nakagami-m quantile function by dint of the product of a power function and an exponential function. Finally, we acquire the proposed expression (8). Comparing (8) with (11), we abandon the first exponential function and replace the constant k_1 in (11) with a power function. The first exponential function rarely contributes to the deviation compensation in fact, and it can be merged with the second exponential function into one, which is simpler. Another drawback is the existence of the constant k_3. We can see from Figure 1(b) that the values of the Nakagami-m quantile function gradually decrease to zero when the values of Nakagami-m CDF decrease from 1 to 0. However, $F^{-1}_{K_{(\text{proposed})}}(0) = k_3$ for (11), which means that the constant blocks the tendency, and this flaw can be observed in the simulation results of [5, 6]. The expression we propose meets this requirement $F^{-1}_{S_{(\text{proposed})}}(0) = 0$, and the excellent performance will be presented in Section 5.

4.2. Approximation for Nakagami-m Quantile Function Based on GO-QSSA

4.2.1. Generalized Opposition-Based Quantum Salp Swarm Algorithm. SSA is inspired by salps' swarming behavior [14] and has been used in several aspects including wireless sensor networks [15], feature selection [16–18], parameter estimation [19], and clustering [20]. Salps usually exist in the form of a swarm called salp chain in deep oceans. There are two groups called the leader and followers in the population according to their positions in the salp chain. The first one of the chain is regarded as the leader; yet, the remaining salps of the chain act as followers. The leader guides the swarm to move in the direction to the food source, whereas each follower follows the one in the front of itself. The principle of SSA is quite simple and easy to understand. But the original SSA easily traps into local optimal solutions, which leads to inexact solutions. Another flaw of SSA is that the designed equations rely on the maximum number of iterations severely, which means that SSA needs the maximum number of iterations to be large enough so that it can explore and exploit well in the search space.

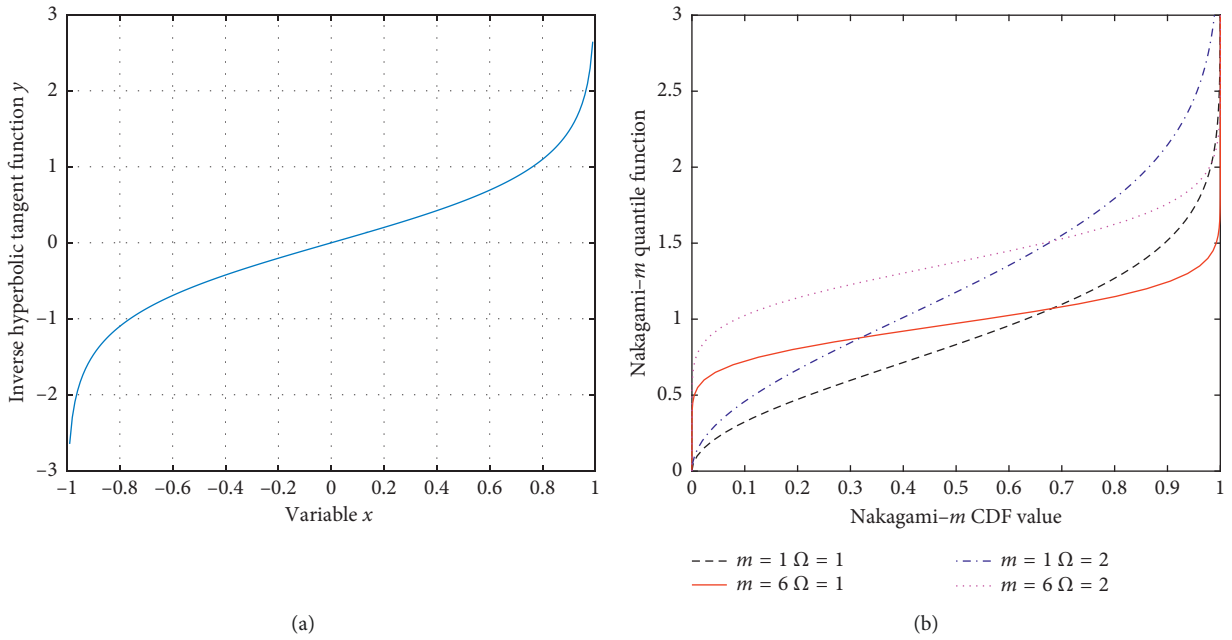

(a) (b)

FIGURE 1: Comparison between the inverse hyperbolic tangent function $y = (1/2)\ln((1+x)/(1-x))$ and Nakagami-m quantile function. Curves of (a) the inverse hyperbolic tangent function and (b) the Nakagami-m quantile function under different parameters.

According to the theory of SSA and quantum computing [21–25], the GO-QSSA is proposed in this paper. The GO-QSSA not only takes advantage of salps' swarm intelligence but also designs brand new mathematical equations to overcome the drawbacks of SSA.

There is a salp swarm containing R salps which possess their own positions. Thus, we define the rth salp's position at tth iteration as $\overline{\mu}_r^t = (\overline{\mu}_{r,1}^t, \overline{\mu}_{r,2}^t, \ldots, \overline{\mu}_{r,D}^t)(r = 1, 2, \ldots, R)$ mapped by the rth salp's quantum position $\mu_r^t = (\mu_{r,1}^t, \mu_{r,2}^t, \ldots, \mu_{r,D}^t)$, where $0 \le \mu_{r,d}^t \le 1 (d = 1, 2, \ldots, D)$ and D is dimension of the salp's position, and it is also the number of coefficients of the proposed expression. The mapping function from a salp's quantum position to its position is defined as follows:

$$\overline{\mu}_{r,d}^t = \overline{\mu}_d^{\text{low}} + \mu_{r,d}^t \cdot \left(\overline{\mu}_d^{\text{high}} - \overline{\mu}_d^{\text{low}}\right), \tag{12}$$

where $\overline{\mu}_{r,d}^t \in [\overline{\mu}_d^{\text{low}}, \overline{\mu}_d^{\text{high}}]$, $\overline{\mu}_d^{\text{low}}$, and $\overline{\mu}_d^{\text{high}}$, respectively, denote the lower and upper bounds of the dth dimension.

The position of each salp denotes a D-dimensional potential solution, and we use the fitness function $F(\overline{\mu}_r^t)$ to evaluate the quality of a potential solution $\overline{\mu}_r^t$ at the tth generation. Meanwhile, the position with best fitness value is regarded as the position of the food source. Here, we use $\overline{\mu}_f^t$ and μ_f^t to denote the food source's position and quantum position, respectively, and we use $\widehat{\mu}_r^t$ to denote the best quantum position that the rth salp acquired by the end of tth iteration.

According to the theory of quantum computing, the quantum rotation angles are updated through quantum positions of the last generation, and then, we use the updated quantum rotation angles to update and get new quantum positions. Meanwhile, considering the structure of the salp chain, the leader should guide the swarm to move in the direction to the food source and the followers follow the one in front of themselves, we propose three strategies to update their quantum rotation angles. The first and second strategies are designed for the leader and can be respectively expressed as

$$\delta_{r,d}^{t+1} = \left(l_1 + l_2 q_{r,d}^t\right) \cdot \left(\mu_{r,d}^t - \mu_{f,d}^t\right) + p_{r,d}^t \cdot \left(\mu_{r,d}^t - \widehat{\mu}_{r,d}^t\right), \tag{13}$$

$$\delta_{r,d}^{t+1} = \left(l_1 + l_2 q_{r,d}^t\right) \cdot \left(\mu_{r,d}^t - \mu_{f,d}^t\right) + p_{r,d}^t \cdot \left(\mu_{r,d}^t - \widehat{\mu}_{v,d}^t\right). \tag{14}$$

In equations (13) and (14), l_1 and l_2 are parameters controlling quantum rotation angles, $q_{r,d}^t$ denotes a random number which is uniformly distributed in $[0, 1]$, $p_{r,d}^t$ denotes a standard normal random number distributed in $[0, 1]$, and v is an random integer generated from $[1, R]$. The leader randomly selects (13) or (14) to update its quantum rotation angles $\delta_{r,d}^t (d = 1, 2, \ldots, D)$. These two strategies are selected by the leader with a probability of 50%. As for followers, we use the third strategy to update their quantum rotation angles. Equations (15) and (16) give the third strategy, we first compute an auxiliary quantum rotation angle $\breve{\delta}_{r,d}^{t+1}$ with (15), and then the quantum rotation angle $\delta_{r,d}^{t+1}$ is the average value of the auxiliary quantum rotation angle $\breve{\delta}_{r,d}^{t+1}$ and the quantum rotation angle of the salp in front of current salp $\delta_{r-1,d}^{t+1}$.

$$\breve{\delta}_{r,d}^{t+1} = q_{r,d}^t \cdot \left(\mu_{r,d}^t - \mu_{f,d}^t\right) + p_{r,d}^t \cdot \left(\mu_{r,d}^t - \widehat{\mu}_{r,d}^t\right), \tag{15}$$

$$\delta_{r,d}^{t+1} = \left(\frac{\breve{\delta}_{r,d}^{t+1} + \delta_{r-1,d}^{t+1}}{2}\right). \tag{16}$$

Here, we have obtained the quantum rotation angles of all salps, and the next step is to update their quantum

positions with equation (17), in which $|\cdot|$ is the absolute value symbol:

$$\mu_{r,d}^{t+1} = \left| \mu_{r,d}^{t} \times \cos\left(\delta_{r,d}^{t+1}\right) - \sqrt{1 - \left(\mu_{r,d}^{t}\right)^2} \times \sin\left(\delta_{r,d}^{t+1}\right) \right|. \quad (17)$$

Opposition-based learning was first proposed to improve algorithms in machine intelligence by Tizhoosh [26], and after that, Wang et al. [27] designed a new scheme called generalized opposition-based learning (GOBL). Researchers have applied these two schemes to several heuristic optimization algorithms since their proposing and have succeeded in improving performance of these algorithms [28–30]. Inspired by GOBL, we propose the corresponding concept in quantum space, GOBL in quantum space, and use it to improve QSSA later. Related definitions are given below.

Definition 1 (opposite point in real-number space). Let $\overline{\mu}_i = (\overline{\mu}_{i,1}, \overline{\mu}_{i,2}, \ldots, \overline{\mu}_{i,D})$ be the ith point in D-dimensional space and $\overline{\mu}_{i,d} \in [\overline{g}_d, \overline{h}_d]\,(d = 1, 2, \ldots, D)$, then the opposite point of $\overline{\mu}_i$ is defined by $\overline{\alpha}_i = (\overline{\alpha}_{i,1}, \overline{\alpha}_{i,2}, \ldots, \overline{\alpha}_{i,D})$, in which $\overline{\alpha}_{i,d}$ is defined as follows:

$$\overline{\alpha}_{i,d} = \overline{g}_d + \overline{h}_d - \overline{\mu}_{i,d}. \quad (18)$$

Definition 2 (GOBL in real number space). Let $\overline{\mu}_i^t = (\overline{\mu}_{i,1}^t, \overline{\mu}_{i,2}^t, \ldots, \overline{\mu}_{i,D}^t)$ be the position of ith individual in the population at the tth generation, $\overline{\mu}_{i,d}^t$ is dth dimension $(d = 1, 2, \ldots, D)$ of $\overline{\mu}_i^t$, then the opposite position of $\overline{\mu}_i^t$ is defined by $\overline{\alpha}_i^t = (\overline{\alpha}_{i,1}^t, \overline{\alpha}_{i,2}^t, \ldots, \overline{\alpha}_{i,D}^t)$, in which $\overline{\alpha}_{i,d}^t$ is defined as follows:

$$\overline{\alpha}_{i,d}^t = k_{i,d}^t \cdot \left(\overline{g}_d^t + \overline{h}_d^t\right) - \overline{\mu}_{i,d}^t. \quad (19)$$

where $k_{i,d}^t$ is a random number uniformly distributed in $[0, 1]$, $\overline{g}_d^t$ and $\overline{h}_d^t$, respectively, denote the minimum and maximum of dth dimension that the the ith candidate solution ever reached by the end of tth generation. Evaluating $\overline{\mu}_i^t$ and $\overline{\alpha}_i^t$, if the fitness of $\overline{\mu}_i^t$ is better than the fitness of $\overline{\alpha}_i^t$, the position of ith individual remains unchanged. Otherwise, the position of ith individual is changed to $\overline{\alpha}_i^t$.

Definition 3 GOBL in quantum space. Let $\mu_i^t = (\mu_{i,1}^t, \mu_{i,2}^t, \ldots, \mu_{i,D}^t)$ be the corresponding quantum position of ith individual's position $\overline{\mu}_i^t = (\overline{\mu}_{i,1}^t, \overline{\mu}_{i,2}^t, \ldots, \overline{\mu}_{i,D}^t)$, $\mu_{i,d}^t \in [0, 1]$, thus the opposite quantum position of μ_i^t is defined by $\alpha_i^t = (\alpha_{i,1}^t, \alpha_{i,2}^t, \ldots, \alpha_{i,D}^t)$, in which $\alpha_{i,d}^t$ is defined as follows:

$$\alpha_{i,d}^t = k_{i,d}^t \cdot \left(g_d^t + h_d^t\right) - \mu_{i,d}^t, \quad (20)$$

where, $k_{i,d}^t$ is a random number uniformly distributed in $[0, 1]$. Here, g_d^t and h_d^t, respectively, denote the minimum and maximum of dth dimension that the ith individual's quantum position ever reached by the end of tth generation and the corresponding opposite position of α_i^t is denoted as $\overline{\alpha}_i^t$. Then, evaluating $\overline{\mu}_i^t$ and $\overline{\alpha}_i^t$, if the fitness of $\overline{\mu}_i^t$ is better than the fitness of $\overline{\alpha}_i^t$, the quantum position of ith individual remains unchanged. Otherwise, the quantum position of ith individual is changed to α_i^t. In GO-QSSA, each individual operates GOBL with a certain probability of P.

4.2.2. GO-QSSA for Approximating Nakagami-m Quantile Function. In this section, we give the method to approximate Nakagami-m quantile function with equation (8) and GO-QSSA. In Section 3.2, we have modelled the approximation problem as optimizing the coefficients of equation (8), and our aim is to get proper coefficients so as to minimize the RMSE, which is a continuous optimization problem. In the GO-QSSA, quantum positions of all salps are updated through their corresponding strategies until the terminating condition is satisfied. The GO-QSSA is summarized as follows.

Step 1. Set the parameters of GO-QSSA: the maximum number of iterations T, the population size R, l_1, l_2, and GOBL probability P.

Step 2. Randomly generate the quantum position of each salp $\mu_r^t = (\mu_{r,1}^t, \mu_{r,2}^t, \ldots, \mu_{r,D}^t)\,(r = 1, 2, \ldots, R)$, $0 \le \mu_{r,d}^t \le 1\,(d = 1, 2, \ldots, D)$ and record the initial quantum position as the local best quantum position $\widehat{\mu}_r^t$ of the rth salp acquired so far. At beginning, set $t = 0$.

Step 3. Evaluate each salp's position with the fitness function $F(\overline{\mu}_r^t)\,(r = 1, 2, \ldots, R)$. Select the position with the best fitness value as the position of food source $\overline{\mu}_f^t$ and record the quantum position of food source μ_f^t.

Step 4. For the leader, update its quantum rotation angles $\delta_{1,d}^t\,(d = 1, 2, \ldots, D)$ and quantum position μ_1^t according to the first or second strategy. For the followers, update their quantum rotation angles $\delta_{r,d}^t\,(r = 2, 3, \ldots, R,\ d = 1, 2, \ldots, D)$ and quantum positions $\mu_r^t\,(r = 2, 3, \ldots, R)$ according to the third strategy.

Step 5. For each salp, generate a number n_r^t which is randomly distributed in $[0, 1]$. If $n_r^t \le P$, then compute its opposite quantum position $\alpha_r^{t+1}\,(r = 1, 2, \ldots, R)$ of the updated quantum position $\mu_r^{t+1}\,(r = 1, 2, \ldots, R)$ with GOBL scheme in quantum space and record its corresponding opposite position $\overline{\alpha}_r^{t+1}\,(r = 1, 2, \ldots, R)$ and position $\overline{\mu}_r^{t+1}\,(r = 1, 2, \ldots, R)$, if $n_r^t > P$, GOBL is not operated for the rth salp.

Step 6. Evaluate each salp's position $\overline{\mu}_r^{t+1}\,(r = 1, 2, \ldots, R)$ and evaluate rth salp's opposite position $\overline{\alpha}_r^{t+1}\,(r = 1, 2, \ldots, R)$ if the rth salp operated GOBL. If the fitness of $\overline{\mu}_r^{t+1}$ is better than the fitness of $\overline{\alpha}_r^{t+1}$, choose μ_r^{t+1} as rth salp's new quantum position. Otherwise, choose α_r^{t+1} as rth salp's new quantum position. Update the quantum position and position of food source if there is a better salp's position. Update $\widehat{\mu}_r^t$.

Step 7. Stop and output the position of food source if $t \ge T$. Otherwise, return to Step 4; meanwhile, set $t = t + 1$.

5. Simulation Results and Discussion

Experiments under several combinations of m and Ω are conducted, and the simulation results show the excellent performance of our approximation against that of the existing approximation methods.

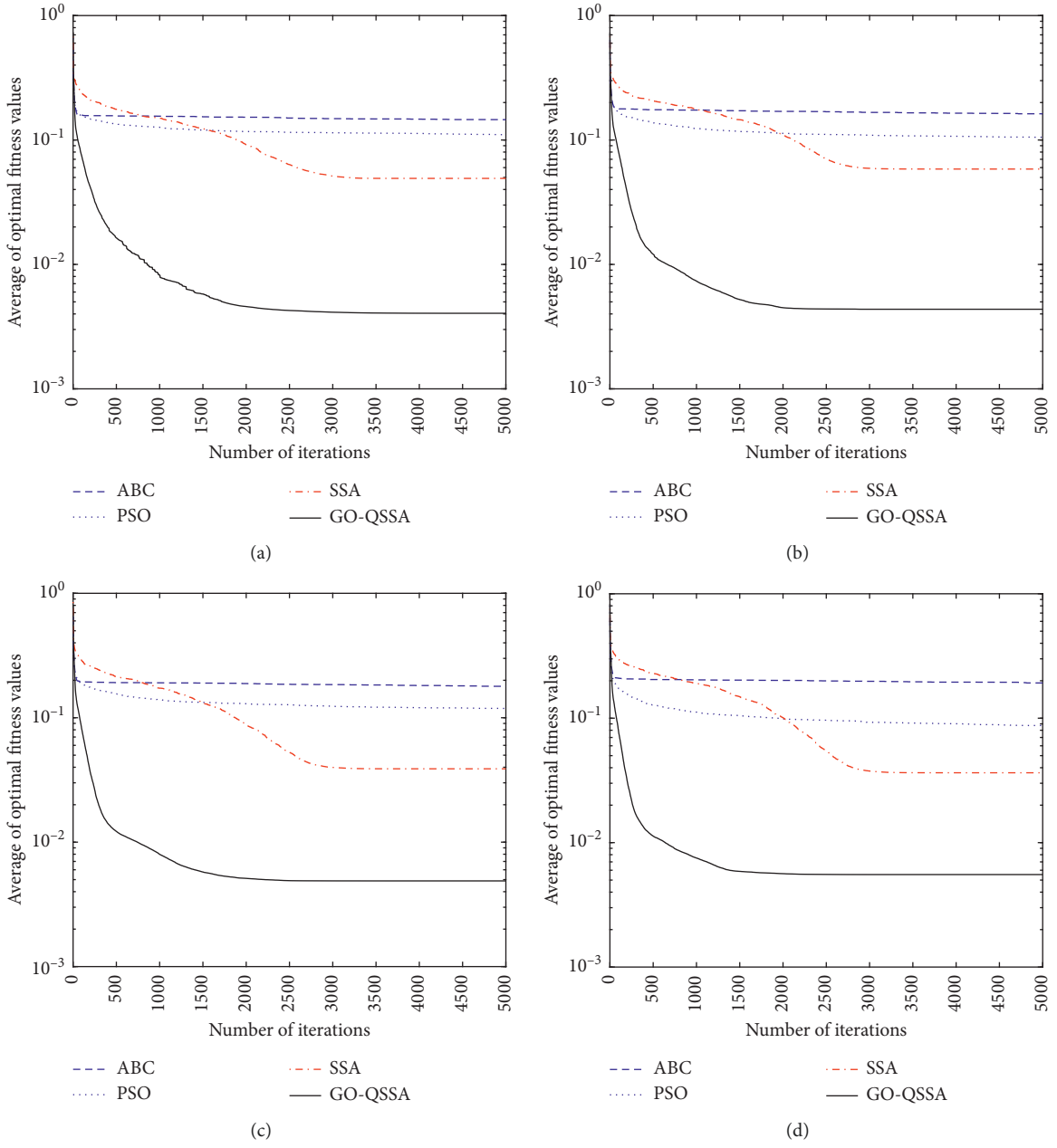

Figure 2: Average of optimal fitness values computed by four algorithms in 100 runs under different fading parameters when $\Omega = 1$. (a) $m = 2.5$. (b) $m = 3.0$. (c) $m = 3.5$. (d) $m = 4.0$.

Here, we give the results optimized by total four algorithms—PSO, ABC, SSA, and GO-QSSA. There are numerous heuristic algorithms in the literature, including cuckoo search algorithm [31, 32], firefly algorithm [33], teaching-learning-based optimization [34], biogeography-based optimization [35], and so on. We choose PSO because it is the most well-known and classic swarm intelligent optimization algorithm, and it has been successfully applied to near all engineering domains. We choose ABC because it is the most efficient algorithm in the publishing literatures when solving this approximation problem. We choose SSA because it is a novel optimization algorithm and has great potentiality to improve the approximation problem of the Nakagami-m model. Compared to PSO, ABC, and SSA, it is easy to understand the superiority of the proposed algorithm in approximating Nakagami-m quantile function. Additionally, PSO is a well-known and classic algorithm based on particle swarm intelligence, ABC is a typical algorithm inspired by the swarm intelligence of bees, and SSA is the source of inspiration of GO-QSSA. The common parameters of the four algorithms are R and T, which are set as 40 and 5,000, respectively. Here, we set T to be large enough to ensure a stable solution is achieved for each algorithm. We set the inertia constant as 1.0, and the two acceleration constants are both equal to 2.0 in PSO, and in GO-QSSA, we set $P = 0.2$, $l_1 = 0.2$, and $l_2 = 0.4$. The parameters of ABC and SSA are the same as in [6, 14], respectively.

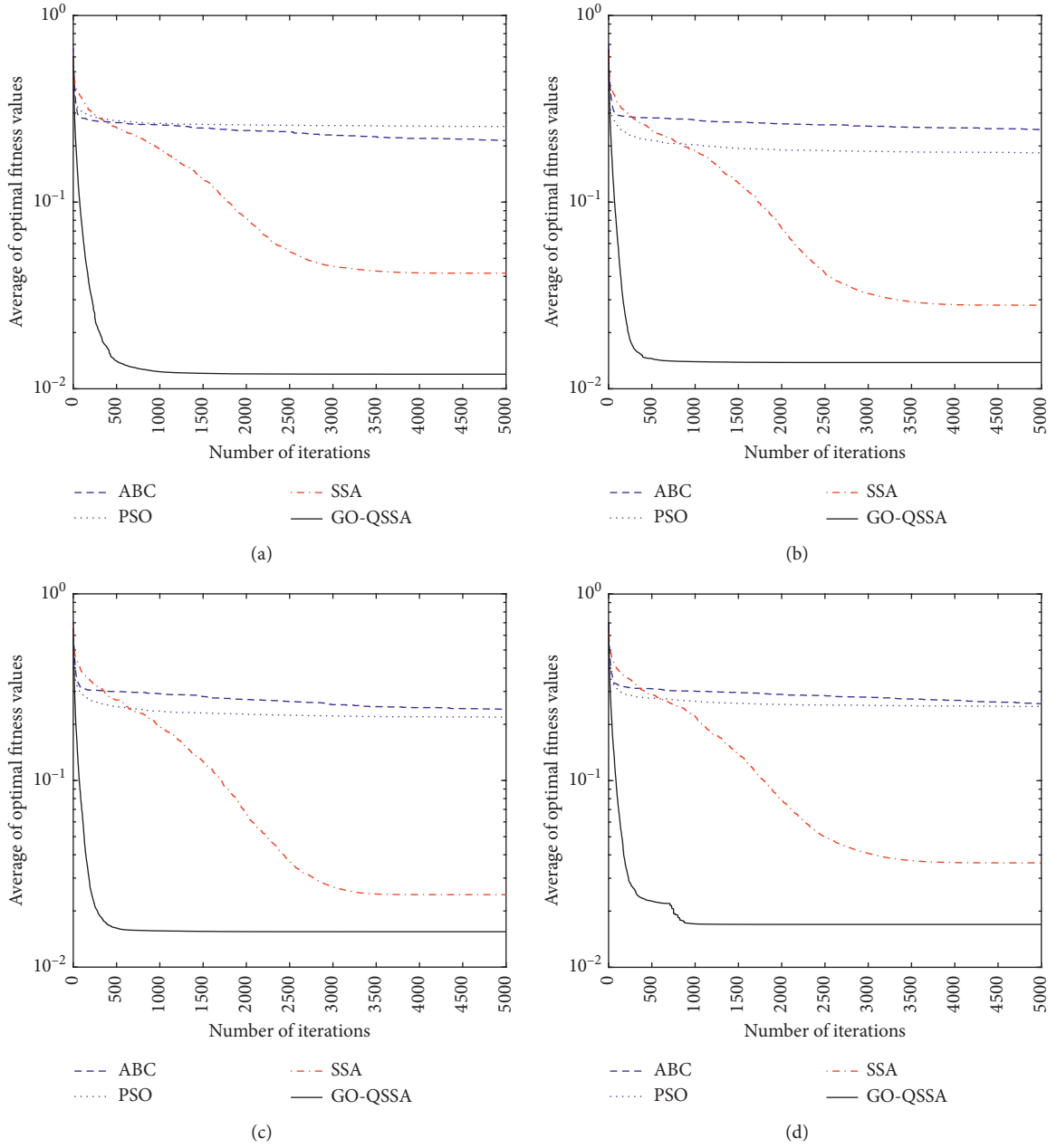

Figure 3: Average of optimal fitness values computed by four algorithms in 100 runs under different fading parameters when $\Omega = 2$. (a) $m = 7.0$. (b) $m = 8.0$. (c) $m = 9.0$. (d) $m = 10.0$.

5.1. Performance of GO-QSSA. In this paper, we conduct independent simulations 100 times for each algorithm under each combination of fading and scale parameters. Convergence curves are shown in Figures 2(a)–2(d) when scaling parameter is set as 1 and fading parameter is set as 2.5, 3.0, 3.5, and 4.0, respectively, and Figures 3(a)–3(d) give convergence curves when scaling parameter is set as 2 and fading parameter is set as 7.0, 8.0, 9.0, and 10.0, respectively. Tables 1 and 2, respectively, give the corresponding statistical data including the minimum, maximum, average, and standard deviation of RMSEs.

As we can see in these figures, PSO and ABC quickly trap into local optimal solutions. There is some probability that SSA can escape from some local optimal solutions, but SSA fails to compute the global optimal solutions in the end. The statistical data in Tables 1 and 2 tell us that the minimum, maximum, and average of RMSEs computed by GO-QSSA are almost on the same level under each combination of fading and scaling parameters, and standard deviation values of RMSEs are much smaller than those of other three algorithms, which means that GO-QSSA can steadily find the best solution. It is obvious that GO-QSSA prevails over ABC, PSO, and SSA in both convergence speed and convergence accuracy, that is to say, GO-QSSA is capable of balancing its exploring and exploiting abilities better than ABC, PSO, and SSA so that it has the ability to jump out of local optima and exploit more in the search space.

Table 1: Statistical comparisons between different algorithms when $\Omega = 1$ and m is set as 2.5, 3.0, 3.5, and 4.0 respectively.

m	Algorithm	Best	Worst	Mean	STD
2.5	PSO	$1.2409E-02$	$2.3049E-01$	$1.1032E-01$	$9.7759E-02$
	ABC	$5.5411E-02$	$1.9640E-01$	$1.4567E-01$	$2.2771E-02$
	SSA	$4.0482E-03$	$2.3033E-01$	$4.9134E-02$	$9.0627E-02$
	GO-QSSA	**4.0482E – 03**	**4.0484E – 03**	**4.0482E – 03**	**2.3611E – 08**
3.0	PSO	$1.5375E-02$	$2.6207E-01$	$1.0526E-01$	$1.0562E-01$
	ABC	$6.9084E-02$	$2.2046E-01$	$1.6213E-01$	$3.0613E-02$
	SSA	$4.3616E-03$	$2.6344E-01$	$5.8407E-02$	$1.0535E-01$
	GO-QSSA	**4.3616E – 03**	**4.3616E – 03**	**4.3616E – 03**	**6.2938E – 10**
3.5	PSO	$1.6453E-02$	$2.8989E-01$	$1.1871E-01$	$1.1737E-01$
	ABC	$1.0771E-01$	$2.3312E-01$	$1.7890E-01$	$2.4986E-02$
	SSA	$4.8817E-03$	$2.8878E-01$	$3.8861E-02$	$9.2479E-02$
	GO-QSSA	**4.8817E – 03**	**4.8817E – 03**	**4.8817E – 03**	**2.2539E – 11**
4.0	PSO	$1.2613E-02$	$3.1806E-01$	$8.7276E-02$	$1.0394E-01$
	ABC	$1.2184E-01$	$2.5891E-01$	$1.9198E-01$	$2.8857E-02$
	SSA	$5.5371E-03$	$3.2140E-01$	$3.6417E-02$	$9.3109E-02$
	GO-QSSA	**5.5371E – 03**	**5.5371E – 03**	**5.5371E – 03**	**1.4481E – 13**

Table 2: Statistical comparisons between different algorithms when $\Omega = 2$ and m is set as 7.0, 8.0, 9.0, and 10.0, respectively.

m	Algorithm	Best	Worst	Mean	STD
7.0	PSO	$1.3551E-02$	$4.1978E-01$	$2.5441E-01$	$1.9053E-01$
	ABC	$7.5002E-02$	$3.1097E-01$	$2.1384E-01$	$5.2317E-02$
	SSA	$1.1977E-02$	$4.1861E-01$	$4.1626E-02$	$1.0410E-01$
	GO-QSSA	**1.1977E – 02**	**1.1977E – 02**	**1.1977E – 02**	**1.2458E – 17**
8.0	PSO	$2.1655E-02$	$4.4409E-01$	$1.8379E-01$	$1.9599E-01$
	ABC	$9.0083E-02$	$3.2507E-01$	$2.4481E-01$	$4.7022E-02$
	SSA	$1.3828E-02$	$4.4421E-01$	$2.8054E-02$	$7.3801E-02$
	GO-QSSA	**1.3828E – 02**	**1.3828E – 02**	**1.3828E – 02**	**3.3420E – 17**
9.0	PSO	$2.0526E-02$	$4.6547E-01$	$2.1849E-01$	$2.1072E-01$
	ABC	$7.7279E-02$	$3.4422E-01$	$2.4093E-01$	$5.7204E-02$
	SSA	$1.5481E-02$	$4.6437E-01$	$2.4459E-02$	$6.3161E-02$
	GO-QSSA	**1.5481E – 02**	**1.5481E – 02**	**1.5481E – 02**	**3.8550E – 17**
10.0	PSO	$2.2120E-02$	$4.8394E-01$	$2.4978E-01$	$2.2095E-01$
	ABC	$1.2149E-01$	$3.8000E-01$	$2.5844E-01$	$5.5310E-02$
	SSA	$1.6970E-02$	$4.8273E-01$	$3.6282E-02$	$9.1703E-02$
	GO-QSSA	**1.6970E – 02**	**1.6970E – 02**	**1.6970E – 02**	**2.0463E – 17**

Table 3: Comparison between our proposed approximation and existing approximations based on curve-fitting under different fading parameters when $\Omega = 1$.

m	Bilim and Develi [4]	Kabalci [5]	Kabalci [6]	Proposed
0.5	0.0572	0.0213	0.0333	6.2606E – 4
0.6	0.0554	0.0153	0.0258	1.2451E – 3
0.7	0.0520	0.0102	0.0245	1.9087E – 3
0.8	0.0512	0.0073	0.0156	2.4405E – 3
0.9	0.0503	0.0076	0.0169	2.8529E – 3
1.0	0.0489	0.0098	0.0161	3.1685E – 3
1.5	0.0438	0.0189	0.0206	3.8556E – 3
2.0	0.0398	0.0217	0.0226	3.9459E – 3
2.5	0.0385	0.0228	0.0230	4.0482E – 3
3.0	0.0355	0.0234	0.0240	4.3616E – 3
3.5	0.0334	0.0237	0.0243	4.8817E – 3
4.0	0.0322	0.0240	0.0254	5.5371E – 3
5.0	0.0306	0.0243	0.0252	7.0110E – 3
6.0	0.0294	0.0245	0.0250	8.4937E – 3
7.0	0.0278	0.0247	0.0248	9.8905E – 3
8.0	0.0261	0.0248	0.0250	1.1179E – 2
9.0	0.0322	0.0250	0.0255	1.2359E – 2
10.0	0.0289	0.0251	0.0256	1.3440E – 2

Table 4: Comparison between our proposed approximation and existing approximations based on curve-fitting under different fading parameters when $\Omega = 2$.

m	Bilim and Develi [4]	Kabalci [5]	Kabalci [6]	Proposed
0.5	0.0829	0.0301	0.0429	1.6811E – 4
0.6	0.0805	0.0216	0.0274	7.1155E – 4
0.7	0.0743	0.0145	0.0246	1.3029E – 3
0.8	0.0719	0.0104	0.0278	1.7516E – 3
0.9	0.0713	0.0108	0.0271	2.0812E – 3
1.0	0.0716	0.0139	0.0294	2.3099E – 3
1.5	0.0606	0.0268	0.0320	2.3751E – 3
2.0	0.0575	0.0307	0.0320	1.5034E – 3
2.5	0.0531	0.0323	0.0326	9.5815E – 4
3.0	0.0505	0.0331	0.0343	1.9993E – 3
3.5	0.0475	0.0336	0.0344	3.4285E – 3
4.0	0.0456	0.0339	0.0355	4.8606E – 3
5.0	0.0517	0.0343	0.0347	7.5286E – 3
6.0	0.0407	0.0347	0.0354	9.8914E – 3
7.0	0.0519	0.0349	0.0360	1.1977E – 2
8.0	0.0475	0.0352	0.0362	1.3828E – 2
9.0	0.0427	0.0354	0.0357	1.5481E – 2
10.0	0.0404	0.0356	0.0358	1.6970E – 2

Table 5: Coefficients of the proposed expression computed by GO-QSSA when the fading parameter m varies from 0.5 to 10 and the scaling parameter Ω is set to 1.

m	a	b	c	d
0.5	0.8177	0.3688	0.9329	0.3072
0.6	0.7495	0.4459	0.6658	0.2240
0.7	0.6945	0.5333	0.5653	0.1213
0.8	0.6469	0.6016	0.5027	0.0649
0.9	0.6053	0.6529	0.4565	0.0367
1.0	0.5690	0.6915	0.4197	0.0244
1.5	0.4401	0.7884	0.3048	0.0388
2.0	0.3618	0.8232	0.2423	0.0735
2.5	0.3090	0.8389	0.2022	0.1027
3.0	0.2708	0.8470	0.1741	0.1257
3.5	0.2417	0.8516	0.1532	0.1439
4.0	0.2187	0.8543	0.1370	0.1587
5.0	0.1845	0.8571	0.1134	0.1810
6.0	0.1602	0.8582	0.0970	0.1971
7.0	0.1418	0.8587	0.0848	0.2093
8.0	0.1274	0.8588	0.0755	0.2188
9.0	0.1157	0.8588	0.0680	0.2265
10.0	0.1061	0.8587	0.0620	0.2328

Table 6: Coefficients of the proposed expression computed by GO-QSSA when the fading parameter m varies from 0.5 to 10 and the scaling parameter Ω is set to 2.

m	a	b	c	d
0.5	1.1043	0.5072	0.8819	0.4577
0.6	0.9166	0.7319	0.5434	0.2766
0.7	1.1486	0.7440	0.5821	-0.2042
0.8	0.8466	0.8224	0.4835	0.2209
0.9	0.7872	0.8912	0.4393	0.1898
1.0	0.7361	0.9436	0.4041	0.1730
1.5	0.5602	1.0786	0.2943	0.1656
2.0	0.4559	1.1293	0.2342	0.1860
2.5	0.3861	1.1531	0.1957	0.2063
3.0	0.3358	1.1660	0.1686	0.2234
3.5	0.2977	1.1736	0.1484	0.2375
4.0	0.2677	1.1785	0.1327	0.2491
5.0	0.2233	1.1841	0.1099	0.2670
6.0	0.1919	1.1870	0.0940	0.2799
7.0	0.1685	1.1888	0.0823	0.2896
8.0	0.1502	1.1901	0.0733	0.2971
9.0	0.1357	1.1909	0.0661	0.3031
10.0	0.1237	1.1916	0.0602	0.3080

5.2. Efficiency of the Proposed Expression. Another main aspect in the approximation problem is the expression for approximating Nakagami-m quantile function. Here, the comparisons of the performance of the proposed expression with that of the existing expressions are shown in Tables 3 and 4, from which we can see that, compared with the results in [4–6], the proposed expression decreases the RMSEs by roughly one order of magnitude in most cases ($m \leq 7$) and even higher in some cases ($m = 0.5$). Lower RMSEs of the proposed expression mean that the proposed expression is capable of fitting the curve of Nakagami-m quantile function much better than those expressions in [4–6]. Meanwhile, Tables 3 and 4 reveal that for a certain scaling parameter such as $\Omega = 1$ or $\Omega = 2$, the RMSE increases when the fading parameter grows, which means that the difficulty of fitting the curve of Nakagami-m quantile function increases as the fading parameter m grows.

Considering the simulation results and analyses above, we finally compute the coefficients of the proposed expression with the assistance of GO-QSSA. The coefficients of the proposed expression computed by GO-QSSA under various scaling parameters ($\Omega = 1$ and $\Omega = 2$) and fading parameters varying from 0.5 to 10 are shown in Tables 5 and 6. In order to show the results more intuitively, comparisons between the approximated values of the proposed expression with coefficients shown in Tables 5 and 6 and the exact values under different fading and scaling parameters are depicted in Figures 4(a)–4(d), from which we can see that our approximation has much lower biases compared with the results in [4–6] under the same parameters. That is to say,

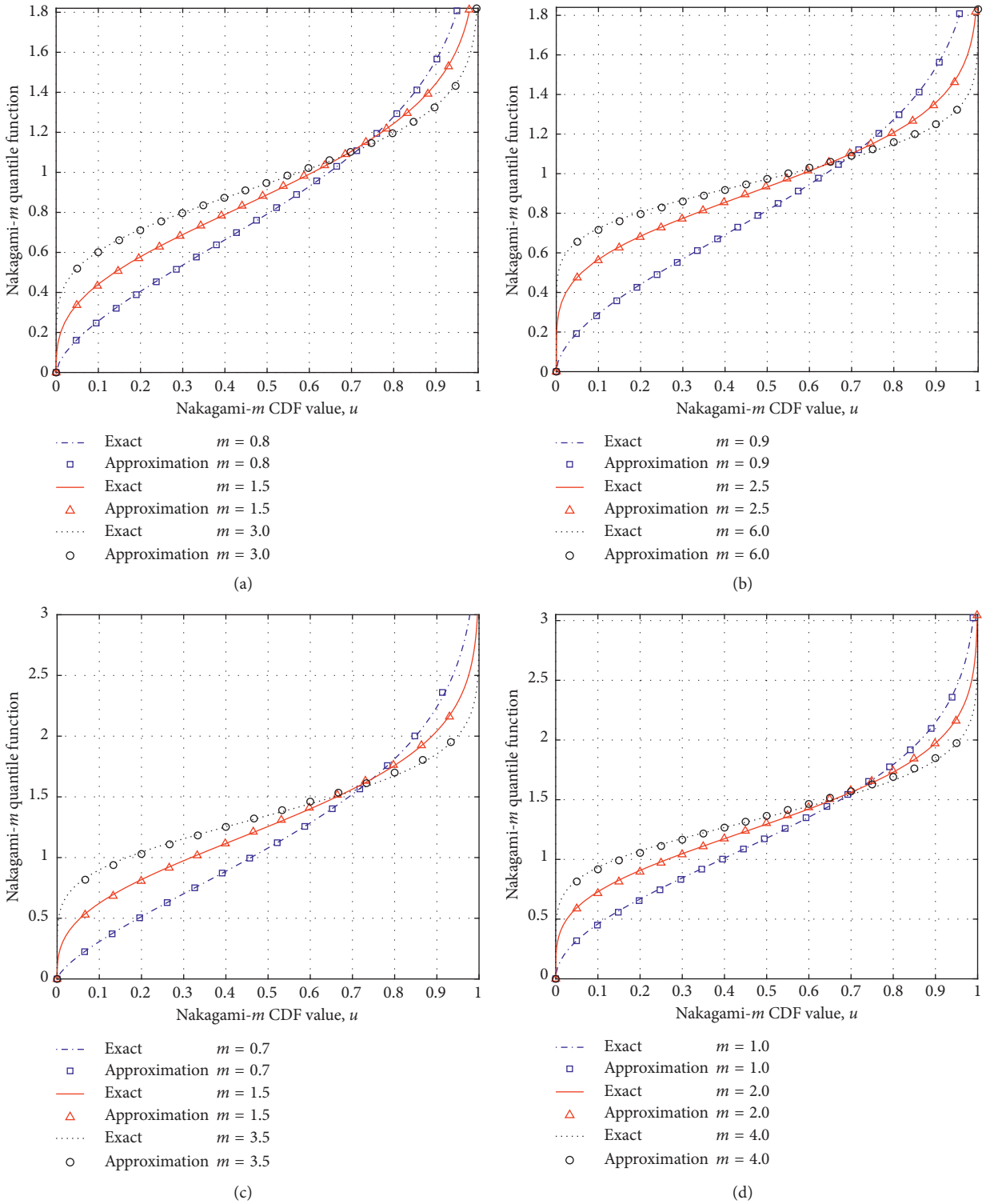

Figure 4: Comparisons between values of the proposed expression and the exact values under different fading and scaling parameters. (a) Comparisons when the fading parameter is set as 0.8, 1.5, and 3.0 and scaling parameter is 1. (b) Comparisons when the fading parameter is set as 0.9, 2.5, and 6.0 and scaling parameter is 1. (c) Comparisons when the fading parameter is set as 0.7, 1.5, and 3.5 and scaling parameter is 2. (d) Comparisons when the fading parameter is set as 1.0, 2.0, and 4.0 and scaling parameter is 2.

our approach to approximate Nakagmi-m quantile function is more efficient. Additionally, we give the plot of mean approximating error against Nakagami-m CDF value under different parameters in Figure 5. Here, the mean approximating error means the average of the difference between the exact and approximating values of Nakagami-m quantile function. We can see from Figure 5 that the approximating error is higher when $\Omega = 2$ and when u is close

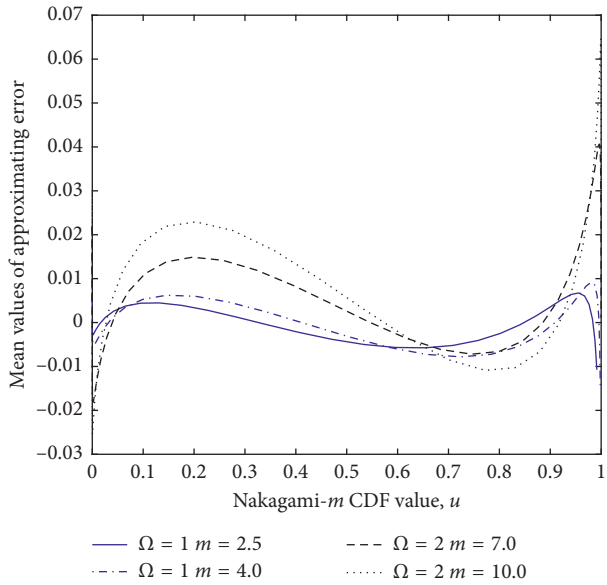

Figure 5: Nakagami-m CDF value against mean approximating error under different parameters.

to 0 or 1, which means that it is more challenging to approximate Nakagami-m quantile function when the scaling parameter increases and when Nakagami-m CDF value is close to 0 or 1.

6. Conclusions

In this paper, a simple and efficient expression for approximating the Nakagami-m quantile function with higher accuracy containing four coefficients is proposed by dint of three elementary functions including an inverse hyperbolic tangent function, an exponential function, and a power function. Then, we combine SSA with quantum swarm intelligence and propose QSSA. Additionally, we expand generalized opposition-based learning strategy from real-number space to quantum space, and we use GO-QSSA to compute coefficients of the proposed expression. Finally, enormous simulation results under different combinations of fading parameters and scaling parameters validate the accuracy of the proposed expression and effectiveness of GO-QSSA.

Data Availability

The data used to support the findings of this study are included within the article.

Conflicts of Interest

The authors declare that they have no conflicts of interest.

Acknowledgments

This research was supported by the National Natural Science Foundation of China (Grant no. 61571149), China Postdoctoral Science Foundation (Grant no. 2015T80325), and Fundamental Research Funds for the Central Universities (HEUCFP201808).

References

[1] M. K. Simon and M. S. Alouini, *Digital Communication over Fading Channels*, Wiley, New Jersey, NY, USA, 2nd edition, 2005.

[2] K. A. Stewart, G. P. Labedz, and K. Sohrabi, "Wideband channel measurements at 900 MHz," in *Proceedings of the 1995 IEEE 45th Vehicular Technology Conference. Countdown to the Wireless Twenty-First Century*, pp. 25–28, IEEE, Chicago, IL, USA, July 1995.

[3] G. L. Stüber, *Principles of Mobile Communication*, Springer, New York, NY, USA, 2nd edition, 2002.

[4] M. Bilim and I. Develi, "A new Nakagami-m inverse CDF approximation based on the use of genetic algorithm," *Wireless Personal Communications*, vol. 83, no. 3, pp. 2279–2287, 2015.

[5] Y. Kabalci, "On the Nakagami-m inverse cumulative distribution function: closed-form expression and its optimization by backtracking search optimization algorithm," *Wireless Personal Communications*, vol. 91, no. 1, pp. 1–8, 2016.

[6] Y. Kabalci, "An improved approximation for the Nakagami-m inverse CDF using artificial bee colony optimization," *Wireless Networks*, vol. 24, no. 2, pp. 663–669, 2018.

[7] A. Abdi and M. Kaveh, "Performance comparison of three different estimators for the Nakagami m parameter using Monte Carlo simulation," *IEEE Communications Letters*, vol. 4, no. 4, pp. 119–121, 2000.

[8] M. Das, B. Sahu, and U. Bhanja, "Coverage analysis of mobile network in Nakagami fading channel," *Wireless Personal Communications*, vol. 97, no. 2, pp. 3261–3276, 2017.

[9] N. C. Beaulieu and C. Cheng, "Efficient Nakagami-m fading channel simulation," *IEEE Transactions on Vehicular Technology*, vol. 54, no. 2, pp. 413–424, 2005.

[10] V. V. Chetlur and H. S. Dhillon, "Downlink coverage analysis for a finite 3-D wireless network of UAV," *IEEE Transactions on Communications*, vol. 65, no. 10, pp. 4543–4558, 2017.

[11] T. Hou, X. Sun, and Z. Song, "Outage performance for non-orthogonal multiple access with fixed power allocation over Nakagami-m fading channels," *IEEE Communications Letters*, vol. 22, no. 4, pp. 744–747, 2018.

[12] N. P. Le, "Throughput analysis of power-beacon-assisted energy harvesting wireless systems over non-identical Nakagami-m fading channels," *IEEE Communications Letters*, vol. 22, no. 4, pp. 840–843, 2017.

[13] S. K. Bandari, V. M. Vakamulla, and A. Drosopoulos, "GFDM/OQAM performance analysis under Nakagami fading channels," *Physical Communication*, vol. 26, pp. 162–169, 2018.

[14] S. Mirjalili, A. H. Gandomi, S. Z. Mirjalili, S. Saremi, H. Faris, and S. M. Mirjalili, "Salp swarm algorithm: a bio-inspired optimizer for engineering design problems," *Advances in Engineering Software*, vol. 114, pp. 163–191, 2017.

[15] H. M. Kanoosh, E. H. Houssein, and M. M. Selim, "Salp swarm algorithm for node localization in wireless sensor networks," *Journal of Computer Networks and Communications*, vol. 2019, Article ID 1028723, 12 pages, 2019.

[16] A. E. Hegazy, M. A. Makhlouf, and G. S. El-Tawel, "Feature selection using chaotic salp swarm algorithm for data classification," *Arabian Journal for Science and Engineering*, vol. 44, no. 4, pp. 3801–3816, 2019.

[17] G. I. Sayed, G. Khoriba, and M. H. Haggag, "A novel chaotic salp swarm algorithm for global optimization and feature selection," *Applied Intelligence*, vol. 48, no. 10, pp. 3462–3481, 2018.

[18] H. Faris, M. M. Mafarja, A. A. Heidari et al., "An efficient binary salp swarm algorithm with crossover scheme for feature selection problems," *Journal of Intelligent & Fuzzy Systems*, vol. 154, pp. 43–67, 2018.

[19] J. Zhang, Z.-H. Wang, and X. Luo, "Parameter estimation for soil water retention curve using the salp swarm algorithm," *Water*, vol. 10, no. 6, p. 815, 2018.

[20] S. K. Majhi, S. Bhatachharya, R. Pradhan, and S. Biswal, "Fuzzy clustering using salp swarm algorithm for automobile insurance fraud detection," *Journal of Intelligent & Fuzzy Systems*, vol. 36, no. 3, pp. 2333–2344, 2019.

[21] H. Gao, S. Zhang, Y. Su, and M. Diao, "Joint resource allocation and power control algorithm for cooperative D2D heterogeneous networks," *IEEE Access*, vol. 7, pp. 20632–20643, 2019.

[22] H. Gao, Y. Du, and C. Li, "Quantum fireworks algorithm for optimal cooperation mechanism of energy harvesting cognitive radio," *Journal of Systems Engineering and Electronics*, vol. 29, no. 1, pp. 18–30, 2018.

[23] H. Gao, S. Zhang, Y. Du, Y. Wang, and M. Diao, "Relay selection scheme based on quantum differential evolution algorithm in relay networks," *KSII Transactions on Internet and Information Systems*, vol. 11, no. 7, pp. 3501–3523, 2017.

[24] W.-P. Ding, C.-T. Lin, M. Prasad, Z. Cao, and J. Wang, "A layered-coevolution-based attribute-boosted reduction using adaptive quantum-behavior PSO and its consistent segmentation for neonates brain tissue," *IEEE Transactions on Fuzzy Systems*, vol. 26, no. 3, pp. 1177–1191, 2018.

[25] Z.-Y. Gao, W.-D. Liu, L.-E. Gao, and F. Zhang, "Path planning method for AUV docking based on adaptive quantum-behaved particle swarm optimization," *IEEE Access*, vol. 7, pp. 78665–78674, 2019.

[26] H. R. Tizhoosh, "Opposition-based learning: a new scheme for machine intelligence," in *Proceedings of the 2005 International Conference on Computational Intelligence for Modelling, Control and Automation (CIMCA 2005)*, pp. 695–701, Vienna, Austria, May 2005.

[27] H. Wang, Z.-J. Wu, S. Rahnamayan, Y. Liu, and M. Ventresca, "Enhancing particle swarm optimization using generalized opposition-based learning," *Information Sciences*, vol. 181, no. 20, pp. 4699–4714, 2011.

[28] Z.-L. Guo, S.-W. Wang, X.-Z. Yue, and H. G. Yang, "Global harmony search with generalized opposition-based learning," *Soft Computing*, vol. 21, no. 8, pp. 2129–2137, 2017.

[29] T. Si, A. De, and A. K. Bhattacharjee, "MRI brain lesion segmentation using generalized opposition-based glowworm swarm optimization," *International Journal of Wavelets, Multiresolution and Information Processing*, vol. 14, no. 5, Article ID 1650041, 2016.

[30] B. Wang, "A novel artificial bee colony algorithm based on modified search strategy and generalized opposition-based learning," *Journal of Intelligent & Fuzzy Systems*, vol. 28, no. 3, pp. 1023–1037, 2015.

[31] H. Wang, W.-J. Wang, H. Sun, Z. Cui, S. Rahnamayan, and S. Zeng, "A new cuckoo search algorithm with hybrid strategies for flow shop scheduling problems," *Soft Computing*, vol. 21, no. 15, pp. 4297–4307, 2017.

[32] M.-Q. Zhang, H. Wang, Z.-H. Cui, and J. Chen, "Hybrid multi-objective cuckoo search algorithm with dynamic local search," *Memetic Computing*, vol. 10, no. 2, pp. 199–208, 2018.

[33] H. Wang, W.-J. Wang, L.-Z. Cui et al., "A hybrid multi-objective firefly algorithm for big data," *Applied Soft Computing*, vol. 69, pp. 806–815, 2018.

[34] R. V. Rao, V. J. Savsani, and D. P. Vakharia, "Teaching-learning-based optimization: a novel method for constrained mechanical design optimization problems," *Computer-Aided Design*, vol. 43, no. 3, pp. 303–315, 2011.

[35] D. Simon, "Biogeography-based optimization," *IEEE Transactions on Evolutionary Computation*, vol. 12, no. 6, pp. 702–713, 2008.